Supplement of Hydrol. Earth Syst. Sci., 27, 213–227, 2023
https://doi.org/10.5194/hess-27-213-2023-supplement

Hydrology and Earth System Sciences
Open Access

Supplement of

Water level variation at a beaver pond significantly impacts net CO_2 uptake of a continental bog

Hongxing He et al.

Correspondence to: Hongxing He (hongxing-he@hotmail.com)

A. Different assumptions to estimate data gaps of the beaver pond water level for 1999-2004 and its implications on the simulated NEE

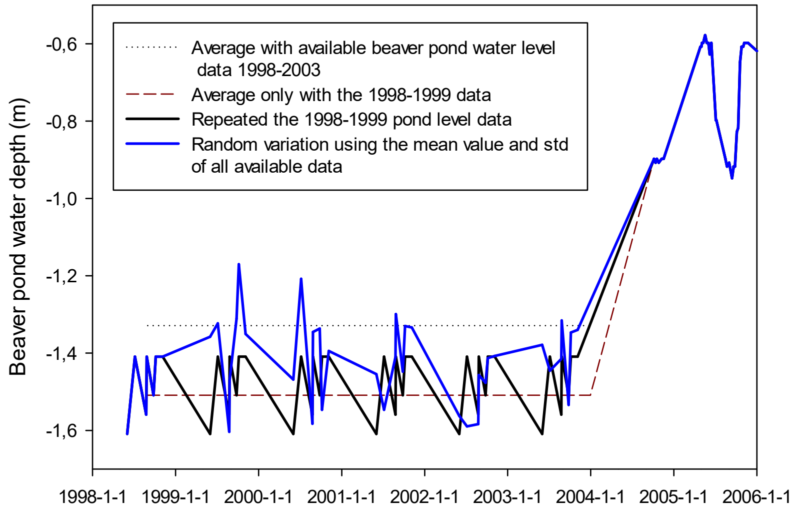

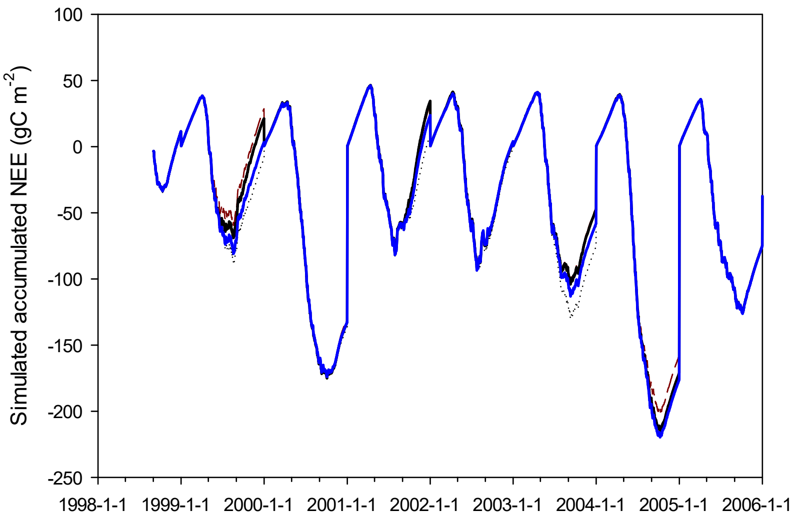

Figure S1: Beaver pond water level (refer to the average peat surface) with four assumptions and the simulated annual accumulated NEEs. Given the minor impacts on the results, the random series was used in the main paper.

B. Brief model descriptions of surface energy fluxes and their partitioning, evapotranspiration and aerodynamic resistance, plant water uptake, soil heat, photosynthesis, and respiration

To solve the peat hydrology, the model needs to estimate evapotranspiration, which is again closely linked to the surface energy partitioning and vegetation characteristics. CoupModel partitioned the energy fluxes according to the surface energy balance (eq.S1). Total net radiation, $R_{n,tot}$ was estimated by both net longwave radiation, i.e. LW_{out} - LW_{in} and short wave incoming radiation R_{is}. The latter R_{is} is one of the forcing variables.

$$\underbrace{\underbrace{\sigma(\varepsilon_s(T_s+273.15)^4}_{LW_{out}} - \underbrace{\varepsilon_a(T_a+273.15)^4)}_{LW_{in}} + (1-a_r)R_{is}}_{R_{n,tot}} = H + LE + q_h + \frac{dF}{dt} \qquad \text{(eq.S1)}$$

Where LW_{out} is the longwave radiation emitted from the ground calculated by using the simulated temperature of the soil surface (beneath the capitulum of the mosses), T_s with consideration of snow surface temperatures in winter. LW_{in} is the incoming longwave radiation from the atmosphere, calculated by using the measured air temperature, T_a. σ is the Stefan-Boltzman constant and the emissivity of the ground, ε_s was assumed to be 1. The emissivity of the atmosphere ε_a was estimated from Konzelmann et al. (1994) function. The surface albedo of ground, a_r is a simulated variable by considering the dynamic area cover of soil, snow, and canopy. Peat soil albedo was assumed to range from 5% (very wet) to 15% (very dry) depending on the soil surface water content (Kellner, 2001). Leaf albedo was set to a constant, 20%, and snow albedo was assumed to be a function of snow age, with 90% for newly formed snow but decreased to 40% after c.a. 1 month time (Gustafsson et al., 2004). Total net radiation is then partitioned into the sensible heat H, latent heat LE and the soil heat flux q_h, respectively. The last term dF/dt is the change in energy storage within the measured reference height and soil surface. Measured energy fluxes data at Mer Bleue show a high energy closure, i.e. 93% in Lafleur et al. (2001). Thus in our modelling study, dF/dt is assumed to be zero.

Beer's law was then applied to partitioning the net radiation between the two vegetation layers and soil surface.

$$R_{ns} = R_{n,tot} e^{-k_{rn} A_l} \qquad \text{(eq.S2)}$$

Where $R_{n,tot}$ is the net radiation above the plant canopy, R_{ns} is the net radiation at the soil surface (beneath the capitulum of the mosses), k_{rn} is an extinction coefficient, assume to be 0.5 and A_l is the leaf area index. The plant intercepted radiation, $R_{n,tot}$ - R_{ns} was then used for calculating the potential evapotranspiration and vegetation growth (see R_n in eq.S3). Given LAI of moss is ~1 in Mer Bleue bog, the light extinction for mosses is nearly complete within a few centimeters thus R_{ns} is very small (Frolking et al., 2002). We thus neglected the potential soil evaporation beneath the mosses induced by R_{ns}.

To calculate evapotranspiration E, CoupModel first calculated the potential evapotranspiration, E_{tp} by using Monteith (1965) equation,

$$E_{tp} = \frac{\Delta R_n + \rho_a c_p \frac{(e_s - e_a)}{r_a}}{\Delta + \lambda(1 + \frac{r_s}{r_a})} \qquad \text{(eq.S3)}$$

Where R_n is net radiation available for evapotranspiration (i.e. $R_{n,tot}$ - R_{ns} in eq.S2), e_s is the vapour pressure at saturation, e_a is the actual vapour pressure, ρ_a is air density, c_p is the specific heat of air at constant pressure, Δ is the slope of saturated vapour pressure versus temperature curve, γ is the psychrometer "constant", r_s is an "effective" surface resistance and r_a is the aerodynamic resistance. The "effective" surface resistance r_s is the result of resistance to evapotranspiration exercised by plant stomata to regulate evaporation by vegetation.

The surface resistance in the leaf r_s in (eq.S3) was calculated using the Lohammar et al. (1980) function of leaf area index A_l, global radiation, R_{is}, and vapour pressure deficit, e_s - e_a,

$$r_s = \frac{1}{A_l \, g_l}$$

$$g_l = \frac{R_{is}}{R_{is} + g_{ris}} \frac{g_{\max}}{1 + \frac{(e_s - e_a)}{g_{vpd}}} \qquad \text{(eq.S4)}$$

Where g_l is stomata conductance, g_{ris} is global radiation intensity that represents half-light saturation in light response and g_{vpd} is vapor pressure deficit that corresponds to half reduction of stomatal conductance, g_{max} is the maximal conductance of fully open stomata for plants. Coefficients of moss surface resistance in the Lohammar equation (Table 1) were derived from previous analysis of evapotranspiration data measured by eddy covariance for bog systems (Kellner, 2001; Wu et al., 2010). In this study, the g_{max} of the shrubs was assumed to be 1.5 times the value of mosses (Table 1).

The aerodynamic resistance r_a in (eq.S3) is calculated by considering two components: One is the aerodynamic resistance as a function of wind speed and temperature gradients; the other is the aerodynamic resistance representing the influence of the vegetation cover. Under neutral conditions, r_a is calculated as,

$$r_a = \frac{\ln^2(\frac{z_{ref} - d}{z_o})}{k^2 u} + r_{alai} A_l \qquad \text{(eq.S5)}$$

Where the measured wind speed, u, is given at the reference measured height, z_{ref}=3 m. k (=0.4) is von Karman's constant, d is the displacement height and z_o is the roughness length. To account for the plant height change with time, roughness length and displacement height were simulated variables, calculated based on the simulated height of each plant individually using the Shaw and Pereira (1982) function.

For the moss layer due to the presence of the above shrub layer, an additional contribution to the aerodynamics resistance, $r_{alai}A_l$ is added in (eq. S5) because of the eventual shadowing of the shrubs. The additional resistance was assumed proportional to the LAI of the shrub layer, with a scale parameter, r_{alai}, (Table 1). Under non-neutral conditions, the first term at the right-hand side of (eq. S5) is further corrected with the Monin-Obukhov stability function (Beljaars and Holtslag, 1991). This involves a dimensionless factor kB^{-1}. In our study, kB^{-1} = 2.3 was obtained from the synthesized value from available measured peatland data (Humphreys et al., 2006).

The actual evapotranspiration E is then calculated as the result of possible stresses at each soil layer depth, plant water uptake characteristics, and for shrubs, also influenced by root distributions (eq.S6). The influencing factors that reduce potential water uptake are drought, a lack of oxygen under water saturation conditions, and soil temperature.

$$E = E_{tp} \int_{z_r}^{0} f(\psi(z)) f(T(z)) r(z) \qquad \text{(eq.S6)}$$

Where for shrubs z_r is the depth with the deepest roots, set to 0.65 m below peat surface according to measured data from Moore et al. (2002). $r(z)$ is the relative root density distribution, set to exponentially decrease with root depth z_r. $f(\psi(z))$, and $f(T(z))$ are response functions for soil water potential, and soil temperature at the modeled soil layer. $f(\psi(z))$ is the water potential response function that regulates the plant water uptake due to either too dry or too wet conditions.

We parameterize the $f(\psi(z))$ in the way that for the shrub layer when the water table is too close to the soil surface, ~ -0.1 m the roots water uptake would start to drop linearly to half of its optimum (i.e. response = 0.5). Moreover, the water uptake drops quickly when the simulated water table is below -0.6 m (Frolking et al., 2002). For the moss layer, no reduction of modeled water uptake occurs when the peatland water table is between ~ -0.4 to -0.1 m but decreases linearly either too dry or too wet. These settings were based on the empirical data from peatland vegetation (e.g. Schipperges and Rydin, 1998; Silvola and Aaltonen, 1984 and William and Flanagan, 1996).

f(T(z)) mimics the reduction of water uptake thus photosynthesis when the soil temperature is low, i.e. in winter. It is an exponential curve that ranges from 0 to 1 with increasing soil temperature. The mosses were assumed to reach optimum at ~ 3 ^{0}C but for the shrubs 15^{0}C (Mellander et al., 2006).

It needs to note the actual evapotranspiration also includes an additional uptake of water by shrub roots in soil layers with no water stress is calculated to compensate for other layers that are exposed to water stress, with a default degree of compensation.

Soil heat flux q_h in eq. (S1) is calculated by mainly considering heat conduction.

$$q_h = -k_h \frac{dT}{dz} \qquad \text{(eq.S7)}$$
$$k_h = h_1 + h_2\theta$$

Where k_h is the thermal conductivity of peat soil calculated by an empirical approach of De Vries (1975), *dT/dz* is the gradient of soil temperature with depth. k_h is assumed proportional to the soil water content, θ, and h_1 and h_2 are parameter values (Table 1).

The snow module of the model followed that of Gustafsson et al. (2001), except the snow melting coefficients for air temperature, M_T, and radiation, M_R (eq 4.33 in pp 194, of Jansson and Karlberg (2011)) is set to three folds of the default melting rate for forests.

Photosynthesis for each plant layer was modeled by a light-use approach (Monteith, 1965) and regulated by water and temperature.

$$C_{atm\to a} = \varepsilon_l \eta f(T_a) f(E/E_{tp}) R_s \qquad \text{(eq.S8)}$$

Where $C_{atm\to a}$ is the total plant growth, R_s is the global radiation absorbed by the canopy (see eq. 4), ε_L is the radiation use efficiency, $f(T_a)$, and $f(E/E_{tp})$ are response functions for temperature, and water. The light use efficiency for shrub and mosses were taken from the estimated value from Kross et al. (2016). The water response is calculated by using (eq.S6). The air temperature response function $f(T_a)$ for photosynthesis was different for the shrub and the moss layer. The shrub layer will start photosynthesis when the air temperature reaches above 5 ^{0}C, and increase linearly to 20 ^{0}C, from 20 to 25 ^{0}C the photosynthesis reaches the maximum, and above 25 ^{0}C photosynthesis decrease linearly and >= 35 ^{0}C the shrub stops its photosynthesis. A similar response function was used for the mosses except the mosses start photosynthesis at 0 ^{0}C, earlier than the shrubs, as been observed in Mer Bleue (Moore et al., 2006). Competition is enabled between the two plant layers for the interception of light with Beer's law and uptake of water.

Decomposition of soil organic matter is calculated by first-order kinetics as,

$$C_{DecompL} = k_l f(T) f(\theta) C_{litter} \qquad \text{(eq. S9)}$$

Where $C_{DecompL}$ is the decomposition rate of soil litter, by changing parameter k_l and pool size C_{litter}, the same equation is used to calculate the decomposition for the other soil organic matters, $f(\theta)$ is the response function for soil moisture, $f(T)$ is the response function for soil temperature, a Q10 temperature function was used. The first-order decay coefficients (Table 1) were set similarly to Frolking et al. (2010). A Q10 value of 3.0 was used (Table 1), according to the fitted value between the measured soil respiration flux and temperature data (Lafleur et al., 2005b). Plant respiration consists of growth respiration and maintenance respiration, where the growth respiration is controlled by recent photosynthesis while maintenance respiration is controlled by standing biomass, both further regulated by a Q10 temperature response function (Jansson and Karlberg, 2011).

C. Parameter values used in the reference model run reported in the main paper

Table S.1 Key model parameters used for the reference run

Symbol	Parameters	Value	Unite	References
n	Coefficient in Van Genuchten function in acrotelm/ catotelm*	1.48/1.28	-	Weiss et al. (1998) Letts et al. (2000)
α	Coefficient in Van Genuchten function	0.123	-	
k_{sat}	Saturated hydraulic conductivity in acrotelm/ catotelm*	10^{-7} to 10^{-3} / 10^{-8} to 10^{-6}	m s^{-1}	Fraser et al., (2001)
a_{surf}	The first-order coefficient for surface runoff	0.8	-	Model default
d_p	Distance between peatland water logger to the beaver pond	250	m	Measured data at Mer Bleue
p_{cmax}	Surface max cover, shrub/moss	1/1	-	Roulet et al. (2007)
k_{rn}	Beer's extinction coefficient	0.5	-	Frolking et al. (2002)
p_{ck}	The sensitivity of reach max cover on LAI, shrub/moss	2/4	-	Moore et al. (2002)
z_r	The lowest shrub rooting depth	0.6	m	Lafleur et al. (2005)
ε	Light use efficiency, shrub/moss	0.7/0.25	g C MJ^{-1}	Kross et al., (2016)
θ_{Amin}	The minimum amount of air that is necessary to prevent a reduction of root water uptake, shrub/moss	35/0.1	vol %	Schipperges and Rydin, (1998); Silvola and Aaltonen, (1984) William and Flanagan, (1996)
ψ_c	Critical pressure head for reduction of potential water uptake, shrub/moss	60/40	cm water	
p_l	Coefficient determines how fast the reduction of potential water uptake when ψ_c is reached, shrub/moss	1/0.3	day^{-1}	
p_{mn}	Threshold Air temperature when photosynthesis starts, shrub/moss	5/0	^0C	Moore et al. 2006
$k_{l,shrub}$	First-order decomposition coefficient for shrub litter	0.32	$year^{-1}$	Frolking et al. (2010)
$k_{l,moss}$	First-order decomposition coefficient for moss litter	0.08	$year^{-1}$	
k_h	First-order decomposition coefficient for refractory organic matter	0.004	$year^{-1}$	
Q_{10}	Q10 value for decomposition	3	-	Lafleur et al., (2005)
$p_{\theta satact}$	Anaerobic activity	0.05	-	Metzger et al. (2015)
z_0	Surface roughness length	0.077	m	(Lafleur et al., 2005a))
kB^{-1}	Difference between the natural logarithm of surface roughness length for momentum and heat	2.3	-	Humphreys et al. (2006)
g_{ris}	Global radiation intensity that represents half-light saturation in light response	553.4	W m^{-2}	Kellner, (2001) Wu et al. (2010)
g_{vap}	Vapor pressure deficit that corresponds to half reduction of stomatal conductance	0.02	kpa	
g_{max}	Maximal conductance of fully open stomata for plants, shrub/moss	0.93/0.62	m s^{-1}	
r_{alai}	LAI Scale factor for r_a of the shrub layer	25	m s^{-1}	Metzger et al. (2015)
h_1	Thermal conductivity coefficient for peat soil	0.06	$Wm^{-1}C^{-1}$	De Vries (1975)
h_2	Thermal conductivity coefficient for peat soil	0.005	$Wm^{-1}C^{-1}$	

* Only mean values or ranges for acrotelm/ catotelm reported. Note overall eight soil layers are modeled for acrotelm and eight layers for catotelm thus coefficients for each layer might differ.

D. Additional measured variables used to validate the model output in the reference run, including energy, hydrological fluxes, and vertical soil temperature profile

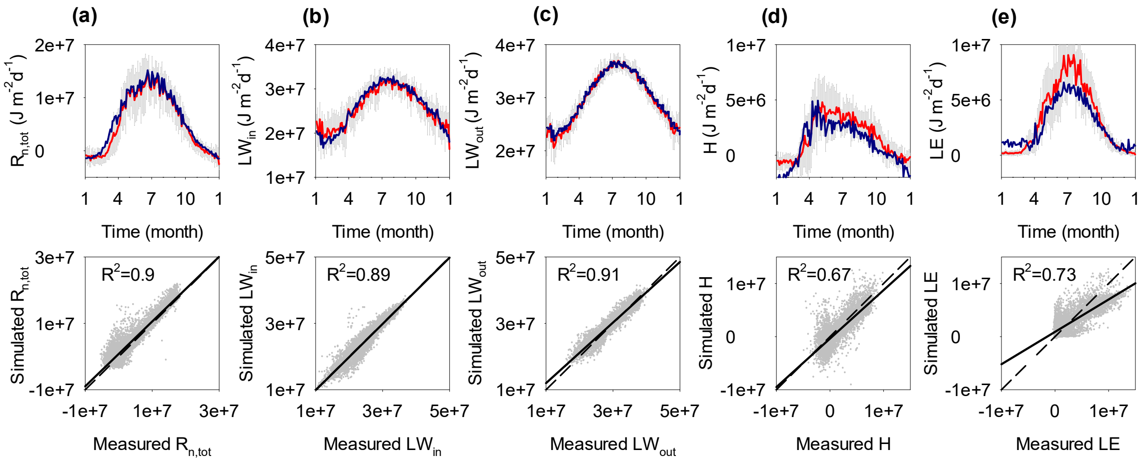

Figure S2: Mean annual seasonal cycle of simulated (blue line) and measured (red line ± standard deviation as grey) fluxes, and scatter plots of simulated vs. measured fluxes: (a) total net radiation $R_{n,tot}$, (b) incoming longwave radiation LW_{in}, (c) outgoing longwave radiation LW_{out}, (d) sensible heat H, and (e) latent heat flux LE. Linear least-squares regressions are fitted to the daily data (black line), 1:1 relationship shown as a faint dotted line, and R^2 denotes the coefficient of determination.

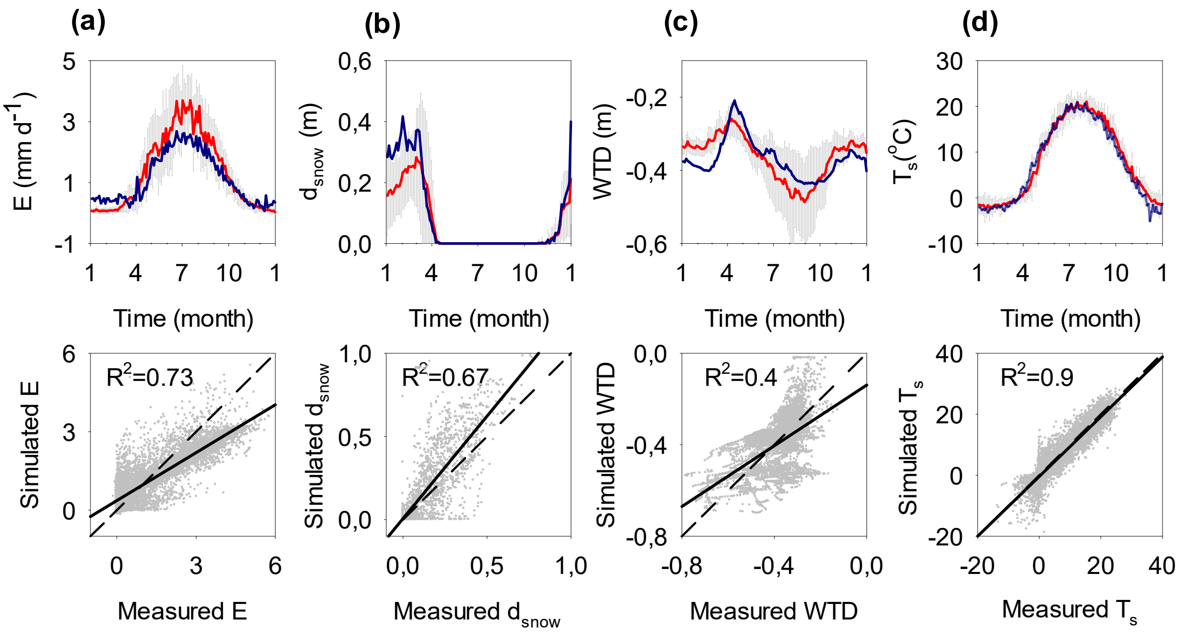

Figure S3: Mean annual seasonal cycle of simulated (blue line) and measured (red line ± standard deviation as grey) fluxes, and scatter plots of simulated vs. measured fluxes: (a) evapotranspiration E, (b) snow depth d_{snow}, (c) peatland water table depth WTD, and (d) soil surface temperature T_s. Linear least-squares regressions are fitted to the daily data (black line), 1:1 relationship shown as a faint dotted line, and R^2 denotes the coefficient of determination.

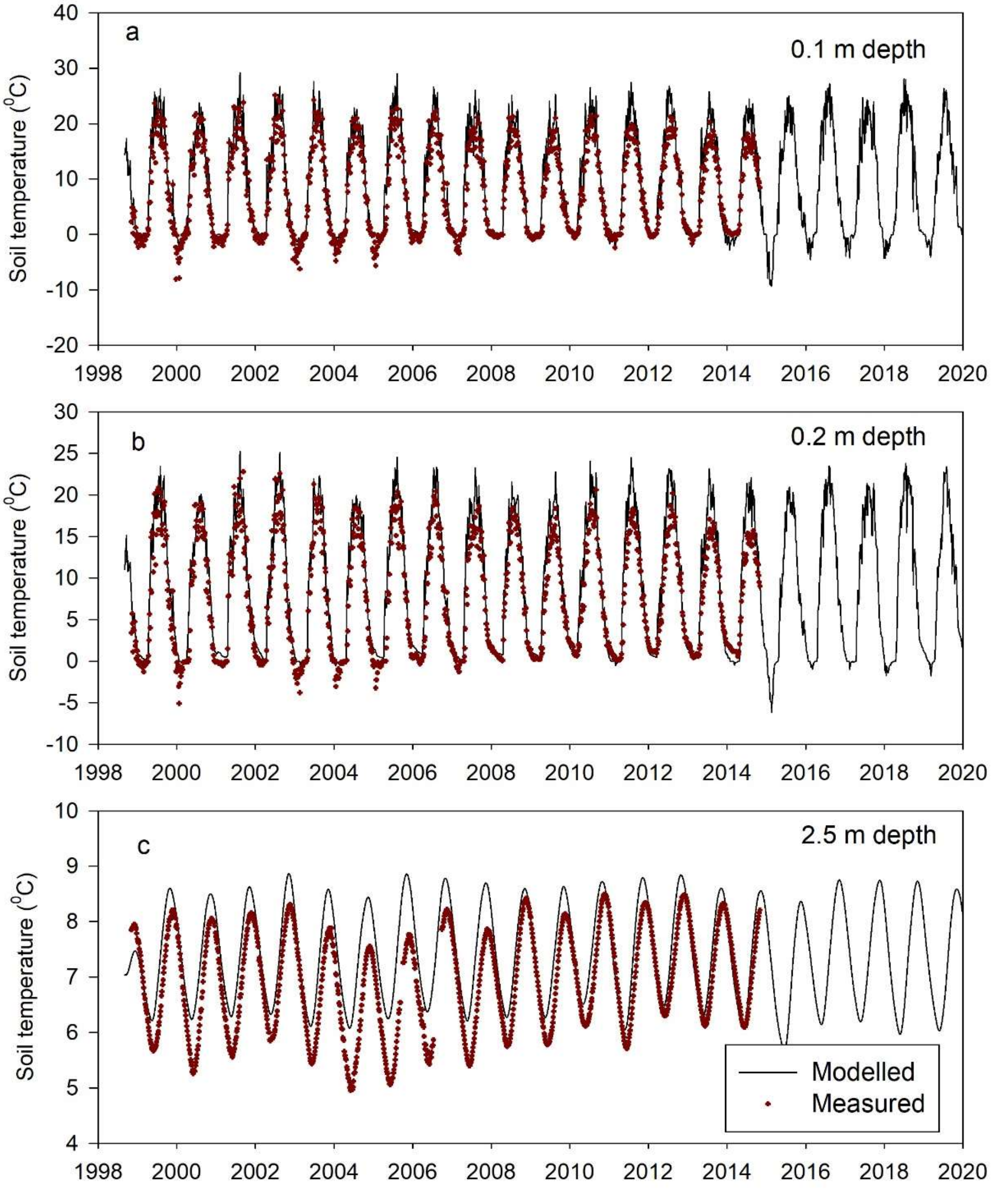

140 **Figure S4 Simulated (line) and measured (dot) vertical soil temperatures at a) 0.1, b) 0.2, and c) 2.5 m depths. For clarity, 5-day averages are shown in the measured data time series.**

E. Brief descriptions of eddy covariance NEE flux processing method and uncertainty

The processing of the 1998-2004 eddy flux data from Mer Bleue was documented in Lafleur et al. (2003) and Roulet et al. (2007). For consistency, we largely retained the flux processing methodology from Roulet et al. (2007) for the 2005-2018 data. The main difference with methods commonly used today (i.e., 2005-2015) and facilitated by LI-COR's EddyPro software is that spectral corrections were not applied. Spectral corrections increase the magnitude of the 30 min fluxes but also add the potential for bias, particularly for shorter towers where closed path instruments and where maximization of the covariance to assess time lags are employed, e.g. (Peltola et al., 2021).

Specifically, using least square linear regression, CO_2 fluxes processed with analytical-only corrections (Moncrieff et al., 2004) and *in-situ* and analytical corrections (Fratini et al., 2012; Horst and Lenschow, 2009) were 1.11 (R^2 = 0.994, RMSE = 0.31 mmol m^{-2} s^{-1}) and 1.08 (R^2 = 0.996, RMSE = 0.23 mmol m^{-2} s^{-1}) times greater than CO_2 fluxes computed with no spectral corrections. In both cases, there was a very small positive offset of 0.06 and 0.01 mmol m^{-2} s^{-1}, respectively. In addition, the gap filling method was updated over years. In Roulet et al. (2007), the gaps of one and two half hours were linearly interpolated, for larger gaps modeled ER and GPP was used (details see NEE subsection under methods of Roulet et al. (2007)). Over years, updated gap filling methods have been applied. This leads to improved annual estimations and the annual average of NEE within the range of ~ ±20 g C m^{-2} yr^{-1} with different gap filling methods. This range is used for defining the accept criteria for GLUE calibration below.

F. Parameter calibration and uncertainty analysis

CoupModel has been applied previously to several boreal peatlands thus parameter uncertainties associated with hydrology and C fluxes were already quantified, e.g., Metzger et al. (2015); Metzger et al. (2016), He et al. (2016) and Kasimir et al. (2021). These studies provide prior information for calibration and uncertainty quantification of the parameters used in this study. However, these earlier studies were conducted on fen peat or restored bogs. We expect the following parameters (Table S.2) at Mer Bleue would differ from the peatlands evaluated before:

The parameters regulating hydrological processes: Saturated hydraulic conductivity (k_{sat}); maximum stomata resistance of shrubs (g_{max}); parameters regulating photosynthesis processes: phenology parameters that regulate the start of photosynthesis (p_{mn} and $TFsum$), the parameter regulating the decrease of photosynthesis under drought or flooded conditions (ψ_c and θ_{Amin}); parameters regulating the ecosystem respiration: the decomposition rate of shrub litter and resistant soil C ($k_{l,\, shrub}$ and k_h), temperature response (t_{Q10}) and soil moisture response for soil C decomposition ($p_{\theta Satact}$, $p_{\theta Low}$ and $p_{\theta Upp}$).

We conducted a covariance-based model parameter calibration using the GLUE approach (He et al., 2016; He et al., 2021). The prior ranges of the parameters were listed in Table S.2 and uniform distributions were assumed. Details of the calibration approach, see He et al. (2016).

Table S.2 Selected parameters and their prior ranges used for the GLUE uncertainty analysis

Parameter name	Unite	Equation	Prior range, minimum	Prior range, maximum
Total hydraulic saturated conductivity, 40-50 cm depth, k_{sat}	mm d^{-1}	1	100	2000
Total hydraulic saturated conductivity, 30-40 cm depth, k_{sat}	mm d^{-1}	1	1000	10000
The maximum stomata conductance, shrub layer, g_{max}	m s^{-1}	S4	0.1	1
The critical water pressure head for reduction of potential water uptake, shrub layer, ψ_c	cm H_2O	S6	40	100
The minimum amount of air that is necessary to prevent any reduced uptake of water from soil, shrub layer, θ_{Amin}	vol %	S6	0.2	0.4
The temperate sum at which the plant recovers from dormancy, shrub layer, *TFsum*	^oC	S8	0.05	1
The minimum mean air temperature for photosynthesis to occur, shrub layer, p_{mn}	^oC	S8	3	6
The microbial activity level under saturation in the soil moisture response function for decomposition, $p_{\theta Satact}$	-	S9	0.025	0.15
The response to a 10 ^oC soil temperature change on microbial activity, t_{Q10}	-	S9	2	4
The water content interval in the soil moisture response function for microbial activity when too dry, $p_{\theta Low}$	vol %	S9	3	20
The water content interval in the soil moisture response function for microbial activity when too wet, $p_{\theta Upp}$	vol %	S9	3	20
The first order rate coefficient for the decay of recalcitrant C, k_h	d^{-1}	S9	5×10^{-6}	5×10^{-5}
The first order rate coefficient for the decay of shrub litter C, $k_{l,\ shrub}$	d^{-1}	S9	2×10^{-4}	0.0015

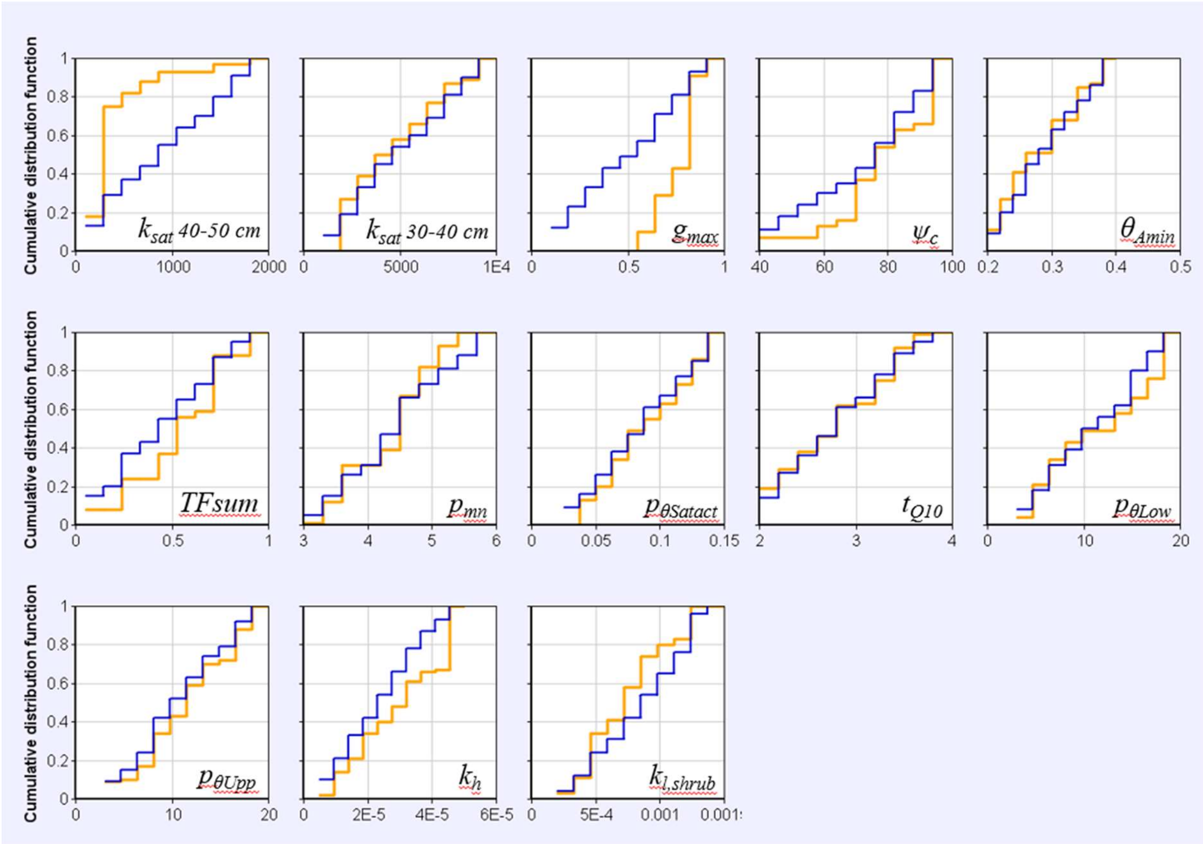

Fig. S5 Cumulative distribution function of calibrated prior (blue) and posterior (orange) parameters, detail of the parameters is given in Table S.2

By random sampling the prior distributions of parameters listed in Table S.2, we made an extra 500 model runs that based on the reference run reported in the main paper. The outputs of each of the 500 model runs were compared with the measured data (Table S.3). The performance indicators, R^2 and ME were used to select the accepted model runs (so called posterior runs). The measurement uncertainty discussed in supplementary section E, ME of ±20 g C m^{-2} yr^{-1} of 1998-2018 NEE, plus a threshold of 0.4 for R^2 of 1998-2018 NEE and WTD were used to define the criteria for model acceptance. Out of the 500 runs, 10 runs were accepted where the ME of the NEE criteria (±20 g C m^{-2} yr^{-1}) reject most of the prior runs. The average NEE simulated in the prior models ranged from -200 to +600 g C m^{-2} yr^{-1}. In the following we report on calibrated posterior parameter distributions and model results. We also rank the parameter sensitivity in controlling the water table and NEE using the posterior model runs.

Fig. S5 shows the shrub maximum stomata conductance, g_{max} and saturated hydraulic conductivity, k_{sat} parameter changed most after the calibration. These highlights the importance of evapotranspiration and lateral drainage processes in regulating the WTD and NEE fluxes for the Mer Bleue system.

Only three parameters show high co-correlations with other parameters after calibration. the temperature response parameter, t_{Q10} and minimum air temperature for photosynthesis to occur, p_{mn} parameter has a correlation coefficient of 0.43. The critical water pressure head for reduction of potential water uptake ψ_c and saturated hydraulic conductivity, k_{sat} at 40-50 cm depth has a correlation coefficient of -0.51. The k_{sat} at 40-50 cm depth and the maximum stomata conductance of the shrub layer, g_{max} has a correlation of 0.3. These inter-correlations highlight the interconnections of the processes within the soil-plant systems.

Table S.3 Correlation table between the posterior parameters and the mean error of the validated variations, bolded values indicate a correlation coefficient >0.4 or <-0.4, thus indicates key regulations on the simulated results

Validated variables	Correlation coefficient between the posterior parameters and the mean error of the simulated variables												
	$p_{\theta Satact}$	t_{Q10}	$p_{\theta Low}$	$p_{\theta Upp}$	k_h	$k_{l,\ shrub}$	g_{max}	k_{sat} 40-50 cm	k_{sat} 30-40 cm	TFsum	p_{mn}	ψ_c	θ_{Amin}
WTD all	0.30	-0.08	0.21	0.03	-0.04	0.24	**-0.69**	**-0.59**	**-0.76**	0.29	-0.21	0.12	0.06
WTD, 1998-2004	0.21	-0.02	0.26	-0.04	0.03	0.34	**-0.84**	**-0.63**	**-0.48**	0.26	-0.17	0.14	-0.02
WTD, 2004-2012	0.36	-0.12	0.16	0.06	-0.07	0.16	**-0.52**	**-0.55**	**-0.89**	0.28	-0.21	0.12	0.10
WTD, 2012-2018	0.27	-0.08	0.21	0.03	-0.03	0.26	**-0.72**	**-0.57**	**-0.74**	0.28	-0.21	0.11	0.06
NEE all	0.15	-0.39	-0.26	0.12	-0.06	**0.69**	-0.35	-0.06	-0.25	-0.06	-0.08	0.08	-0.17
NEE, 1998-2004	0.10	**-0.41**	-0.26	0.18	-0.03	**0.70**	-0.33	-0.01	-0.21	-0.03	-0.11	0.07	-0.22
NEE, 2004-2012	0.15	-0.37	-0.23	0.10	-0.02	**0.68**	-0.32	-0.04	-0.20	-0.07	-0.06	0.07	-0.26
NEE, 2012-2018	0.19	-0.35	-0.25	0.23	-0.02	**0.68**	-0.34	-0.02	-0.22	-0.01	-0.12	-0.01	-0.25
Tota net radaiton	0.27	-0.09	-0.09	0.10	-0.13	-0.28	**0.61**	-0.15	**-0.50**	-0.07	-0.09	0.15	0.02
Outgoing long wave radiation	0.10	-0.02	0.23	-0.03	0.07	0.36	**-0.93**	-0.37	-0.34	0.29	-0.12	-0.02	0.00
Total Sensible flow	0.10	-0.02	0.24	-0.03	0.08	0.35	**-0.93**	-0.37	-0.33	0.29	-0.12	-0.03	-0.02
Total Latent flow	-0.09	0.02	-0.23	0.03	-0.08	-0.36	**0.93**	0.36	0.32	-0.29	0.11	0.03	0.02
Gross Primary Production	-0.08	-0.14	0.15	0.29	0.36	-0.12	0.06	0.26	0.31	0.15	**-0.43**	-0.29	**-0.77**
Ecosystem respiration	0.15	**-0.42**	-0.25	0.14	-0.04	**0.66**	-0.32	-0.02	-0.22	-0.05	-0.11	0.06	-0.24
Evapotranspiration	-0.09	0.02	-0.23	0.03	-0.08	-0.36	**0.93**	0.36	0.32	-0.29	0.11	0.03	0.02
Snow Depth	0.35	-0.11	0.20	0.05	-0.02	0.17	**-0.64**	**-0.51**	**-0.81**	0.35	-0.21	-0.01	0.04
Soil Temperature 10 cm	0.29	-0.02	0.11	0.04	-0.02	0.07	-0.36	**-0.67**	**-0.57**	0.20	-0.16	0.26	0.10
Soil Temperature 20 cm	0.10	0.11	0.07	0.13	-0.01	0.13	-0.38	-0.21	-0.29	0.21	-0.02	0.05	0.04
Soil Temperature 250 cm	0.01	0.12	0.03	0.14	-0.01	0.16	-0.39	-0.01	-0.16	0.18	0.04	-0.02	0.08

The parameter sensitivity ranking shown in the Table S.3 indicate that WTD at the Mer Bleue bog were mainly regulated by g_{max} (regulating evapotranspiration) and k_{sat} (regulating lateral drainage to BP), and the NEE were mainly regulated by the decomposition of the shrub litter soil C, $k_{l,\ shrub}$ (mainly regulating ecosystem respiration)

More importantly, the controlling parameters of the WTD and NEE stayed the same over the different BP disturbance phases. Table S.3 also shows the key regulations of other variables validated in our reference runs, thus this information provides key insights into future modeling of continental bogs.

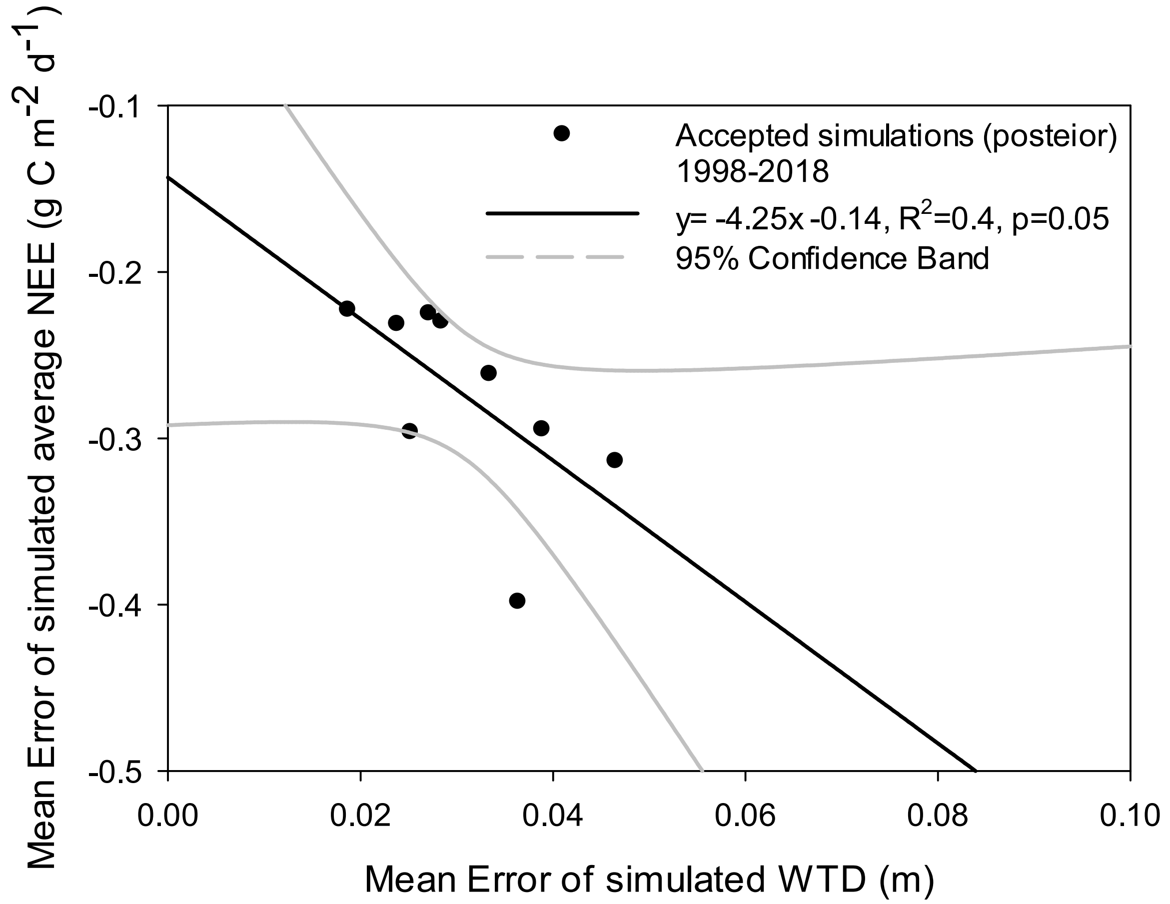

Fig. S6 Relationship between the mean error of simulated WTD and NEE (1998-2018). The dots are accepted model simulations thus the variations are created by the posterior parameter ranges (i.e., parameter uncertainties)

We further show the relationships between the simulated WTD and NEE within the posterior model runs (Fig. S6). Each dots represent the mean error (i.e., average biases) of NEE and WTD over 1998-2018. Note the annual average is used in Fig. S6, compared to the growing season only in Fig. 8 in the main paper. The key message is even considering the uncertainties by the model parameters (Table S.3, Fig. S5, S6) WTD still dominants the control of NEE, as shown by our reference runs in the main paper.

References

Beljaars, A. C. M. and Holtslag, A. A. M.: Flux parameterization over land surfaces for atmospheric models, Journal of Applied Meteorology, 30, 327-341, 1991.

de Vries, D. A.: Heat transfer in soils, in: Heat and Mass Transfer in the biosphere. I. transfer processes in plant environment, edited by: de Vries, D. A., and Afgan, N. F., Wiley, New York, 5-28, 1975.

Fratini, G., Ibrom, A., Arriga, N., Burba, G., and Papale, D.: Relative humidity effects on water vapour fluxes measured with closed-path eddy-covariance systems with short sampling lines, Agricultural and Forest Meteorology, 165, 53-63, 10.1016/j.agrformet.2012.05.018, 2012.

Frolking, S., Roulet, N. T., Moore, T. R., Lafleur, P. M., Bubier, J. L., and Crill, P. M.: Modeling seasonal to annual carbon balance of Mer Bleue Bog, Ontario, Canada, Global Biogeochemical Cycles, 16, 4-1-4-21, 10.1029/2001gb001457, 2002.

Frolking, S., Roulet, N. T., Tuittila, E., Bubier, J. L., Quillet, A., Talbot, J., and Richard, P. J. H.: A new model of Holocene peatland net primary production, decomposition, water balance, and peat accumulation, Earth System Dynamics Discussions, 1, 115-167, 10.5194/esdd-1-115-2010, 2010.

Gustafsson, D., Lewan, E., and Jansson, P. E.: Modelling water and heat balance of boreal landscape, comparison of forest and arable land in Scandinavia, Journal of Applied Meteorology, 43, 1750-1767, 2004.

Gustafsson, D., Stähli, M., and Jansson, P.-E.: The surface energy balance of a snow cover: comparing measurements to two different simulation models, Theoretical and Applied Climatology, 70, 81-96, 2001.

He, H., Jansson, P.-E., and Gärdenäs, A. I.: CoupModel (v6.0): an ecosystem model for coupled phosphorus, nitrogen, and carbon dynamics – evaluated against empirical data from a climatic and fertility gradient in Sweden, Geoscientific Model Development, 14, 735-761, 10.5194/gmd-14-735-2021, 2021.

He, H., Jansson, P.-E., Svensson, M., Meyer, A., Klemedtsson, L., and Kasimir, Å.: Factors controlling Nitrous Oxide emission from a spruce forest ecosystem on drained organic soil, derived using the CoupModel, Ecological Modelling, 321, 46-63, 10.1016/j.ecolmodel.2015.10.030, 2016.

Horst, T. W. and Lenschow, D. H.: Attenuation of Scalar Fluxes Measured with Spatially-displaced Sensors, Boundary-Layer Meteorology, 130, 275-300, 10.1007/s10546-008-9348-0, 2009.

Humphreys, E. R., Lafleur, P. M., Flanagan, L. B., Hedstrom, N., Syed, K. H., Glenn, A. J., and Granger, R.: Summer carbon dioxide and water vapor fluxes across a range of northern peatlands, Journal of Geophysical Research: Biogeosciences, 111, 10.1029/2005jg000111, 2006.

Jansson, P.-E. and Karlberg, L.: User manual of Coupled heat and mass transfer model for soil-plant-atmosphere systems, Royal institute of technology, Department of land and water resources, Stockholm2011.

Kasimir, Å., He, H., Jansson, P. E., Lohila, A., and Minkkinen, K.: Mosses are Important for Soil Carbon Sequestration in Forested Peatlands, Frontiers in Environmental Science, 9, 10.3389/fenvs.2021.680430, 2021.

Kellner, E.: Surface energy fluxes and control of evapotranspiration from a Swedish sphagnum mire, Agricultural and Forest Meteorology, 110, 101-123, 2001.

Konzelmann, T., Van de Wal, R. S. W., Greuell, W., Bintanja, R., Henneken, E. A. C., and Abe-Ouchi, A.: Parameterization of global and longwave incoming radiation for the Greenland Ice Sheet, Global and Planetary Change, 9, 143-164, 10.1016/0921-8181(94)90013-2, 1994.

Kross, A., Seaquist, J. W., and Roulet, N. T.: Light use efficiency of peatlands: Variability and suitability for modeling ecosystem production, Remote Sensing of Environment, 183, 239-249, 10.1016/j.rse.2016.05.004, 2016.

Lafleur, P. M., Roulet, N. T., and Admiral, S. W.: Annual cycle of CO2exchange at a bog peatland, Journal of Geophysical Research: Atmospheres, 106, 3071-3081, 10.1029/2000jd900588, 2001.

Lafleur, P. M., Hember, R. A., Admiral, S. W., and Roulet, N. T.: Annual and seasonal variability in evapotranspiration and water table at a shrub-covered bog in southern Ontario, Canada, Hydrological Processes, 19, 3533-3550, 10.1002/hyp.5842, 2005a.

Lafleur, P. M., Moore, T. R., Roulet, N. T., and Frolking, S.: Ecosystem Respiration in a Cool Temperate Bog Depends on Peat Temperature But Not Water Table, Ecosystems, 8, 619-629, 10.1007/s10021-003-0131-2, 2005b.

Lafleur, P. M., Roulet, N. T., Bubier, J. L., Frolking, S., and Moore, T. R.: Interannual variability in the peatland-atmosphere carbon dioxide exchange at an ombrotrophic bog, Global Biogeochemical Cycles, 17, n/a-n/a, 10.1029/2002gb001983, 2003.

Letts, G. M., Roulet, N. T., and Comer, N. T.: Parametrization of peatland hydraulic properties for the Canadian land surface scheme, Atmosphere Ocean, 38, 141-160, 2000.

Lohammar, T., Larsson, S., Linder, S., and Falk, S. O.: FAST-simulation models of gaseous exchange in Scots pine, Structure and function of northern Coniferous forests-an ecosystem study1980.

Mellander, P.-E., Stähli, M., Gustafsson, D., and Bishop, K.: Modelling the effect of low soil temperatures on transpiration by Scots pine, Hydrological processes, 20, 1929-1944, 10.1002/hyp.6045, 2006.

Metzger, C., Nilsson, M. B., Peichl, M., and Jansson, P.-E.: Parameter interactions and sensitivity analysis for modelling carbon heat and water fluxes in a natural peatland, using CoupModel v5, Geoscientific Model Development, 9, 4313-4338, 10.5194/gmd-9-4313-2016, 2016.

Metzger, C., Jansson, P. E., Lohila, A., Aurela, M., Eickenscheidt, T., Belelli-Marchesini, L., Dinsmore, K. J., Drewer, J., van Huissteden, J., and Drösler, M.: CO_2 fluxes and ecosystem dynamics at five European treeless peatlands – merging data and process oriented modeling, Biogeosciences, 12, 125-146, 10.5194/bg-12-125-2015, 2015.

Moncrieff, J., Clement, R., Finnigan, J., and Meyers, T.: Averaging, Detrending, and Filtering of Eddy Covariance Time Series, Handbook of Micrometeorology, Springer, Dordrecht, https://doi.org/10.1007/1-4020-2265-4_2, 2004.

Monteith, J. L.: Evaporation and environment, Symposia society for experimental biology, 16, 205-234, 1965.

Moore, T., Bubier, J., Frolking, S., Lafleur, P. M., and Roulet, N. T.: Plant biomass and production and CO2 exchange in an ombrotrophic bog, Journal of Ecology, 90, 25-36, 2002.

Moore, T. R., Lafleur, P. M., Poon, D. M. I., Heumann, B. W., Seaquist, J. W., and Roulet, N. T.: Spring photosynthesis in a cool temperate bog, Global Change Biology, 12, 2323-2335, 10.1111/j.1365-2486.2006.01247.x, 2006.

Peltola, O., Aslan, T., Ibrom, A., Nemitz, E., Rannik, Ü., and Mammarella, I.: The high-frequency response correction of eddy covariance fluxes – Part 1: An experimental approach and its interdependence with the time-lag estimation, Atmospheric Measurement Techniques, 14, 5071-5088, 10.5194/amt-14-5071-2021, 2021.

Roulet, N. T., Lafleur, P. M., Richard, P. J. H., Moore, T. R., Humphreys, E. R., and Bubier, J.: Contemporary carbon balance and late Holocene carbon accumulation in a northern peatland, Global Change Biology, 13, 397-411, 10.1111/j.1365-2486.2006.01292.x, 2007.
Shaw, R. H. and Pereira, A. R.: Aerodynamic roughness of a plant canopy: a numerical experiment, Agricultural Meteorology, 26, 51-65, 1982.
Wu, J., Kutzbach, L., Jager, D., Wille, C., and Wilmking, M.: Evapotranspiration dynamics in a boreal peatland and its impact on the water and energy balance, Journal of Geophysical Research, 115, 10.1029/2009jg001075, 2010.